Quasi-elastic Scattering

Toshio Yamaguchi
Department of Chemistry, Fukuoka University
yamaguchi@fukuoka-u.ac.jp

The 3rd Neutron and Muon School, 20-24 November 2018, Tokai

Book

Quasielastic neutron scattering – Principles and Applications in Solid State Chemistry, Biology and Material Science

by M Bée

Adam Hilger, Bristol and Philadelphia

ISBN: 0-85274-371-8
IOP Publishing Ltd 1988

The two basic quantities to be measured in a scattering experiment are: (i) the energy transfer, $\hbar\omega$, between the initial, E_0, and final, E, energies of the neutron

$$\hbar\omega = E - E_0 = \frac{\hbar^2}{2m}(k^2 - k_0^2)$$

where k_0 and k are the corresponding wavevectors, and (ii) the scattering vector, Q, corresponding to the wavevector transfer:

$$Q = k - k_0.$$

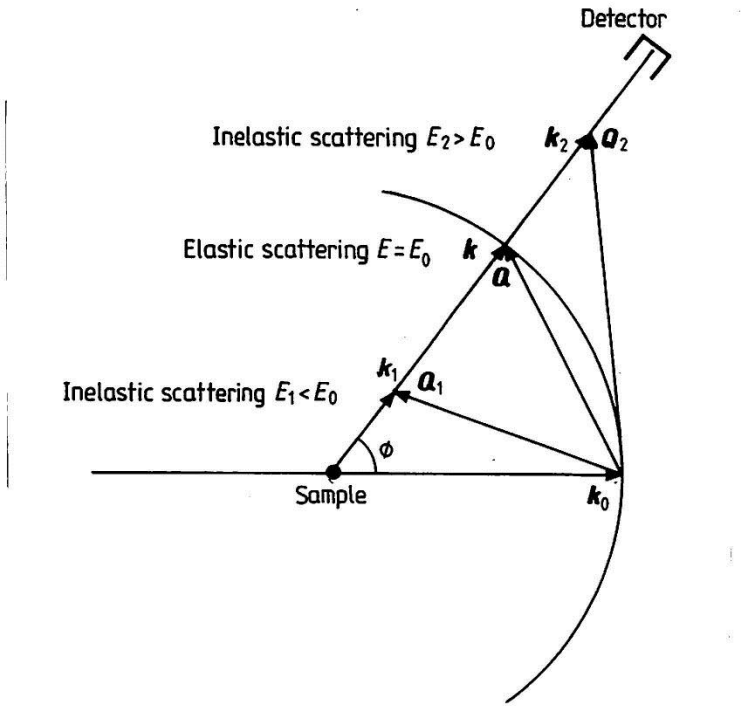

Figure 2.1 Variation of the wavevector transfer $Q = k - k_0$ as a function of the energy transfer $\hbar\omega = E - E_0$ for neutrons detected at constant scattering angle: k_0, incident neutron wavevector; E_0, incident neutron energy; k, k_1, k_2: final neutron wavevectors: E, E_1, E_2: final neutron energies.

scattering lengths

- coherent $b_i^{coh} = \langle b_i \rangle$
- incoherent $b_i^{inc} = [\langle b_i^2 \rangle - \langle b_i \rangle^2]^{1/2}$

cross-sections

$\sigma_{coh}^i = 4\pi\, b_i^2$ coh

$\sigma_{inc}^i = 4\pi\, b_i^2$ inc

	spin	σ_{coh}	σ_{inc}
H	1/2	1.76	79.7
D	1	5.6	2.0

in barn (1 barn = 10^{-24} cm^2)

$$\frac{\partial^2\sigma}{\partial\Omega\partial\omega} = \left(\frac{\partial^2\sigma}{\partial\Omega\partial\omega}\right)_{\text{coh}} + \left(\frac{\partial^2\sigma}{\partial\Omega\partial\omega}\right)_{\text{inc}}$$

$$\left(\frac{\partial^2\sigma}{\partial\Omega\partial\omega}\right)_{\text{coh}} = \frac{1}{N}\frac{k}{k_0}\sum_{\alpha=1}^{n}\sum_{\beta=1}^{n} b_\alpha^{\text{coh}} b_\beta^{\text{coh}} \sqrt{N_\alpha N_\beta}\; S^{\alpha\beta}(\boldsymbol{Q}, \omega)$$

b_α^{coh} and b_β^{coh} are the coherent scattering lengths

$$\left(\frac{\partial^2\sigma}{\partial\Omega\partial\omega}\right)_{\text{inc}} = \frac{1}{N}\frac{k}{k_0}\sum_{\alpha=1}^{n} b_\alpha^{\text{inc}}\, S_{\text{inc}}^{\alpha}(\boldsymbol{Q}, \omega)$$

b_α^{inc} is the incoherent scattering length

$$S^{\alpha\beta}(\boldsymbol{Q}, \omega) = \frac{1}{2\pi\sqrt{N_\alpha N_\beta}} \int_{-\infty}^{\infty} \sum_{i_\alpha=1}^{N_\alpha}\sum_{j_\beta=1}^{N_\beta} \langle \exp\{\mathrm{i}\boldsymbol{Q}\cdot\boldsymbol{R}_{i_\alpha}(t)\} \times \exp\{-\mathrm{i}\boldsymbol{Q}\cdot\boldsymbol{R}_{j_\beta}(0)\}\rangle \exp(-\mathrm{i}\omega t)\,\mathrm{d}t$$

$$S_{\text{inc}}^{\alpha}(\boldsymbol{Q}, \omega) = \frac{1}{2\pi N_\alpha} \int_{-\infty}^{\infty} \sum_{i_\alpha=1}^{N_\alpha} \langle \exp\{\mathrm{i}\boldsymbol{Q}\cdot\boldsymbol{R}_{i_\alpha}(t)\} \times \exp\{-\mathrm{i}\boldsymbol{Q}\cdot\boldsymbol{R}_{i_\alpha}(0)\}\rangle \exp(-\mathrm{i}\omega t)\,\mathrm{d}t$$

$$S^{\alpha\beta}(\boldsymbol{Q}, \omega) = \frac{1}{2\pi}\int_{-\infty}^{\infty} I^{\alpha\beta}(\boldsymbol{Q}, t)\exp(-\mathrm{i}\omega t)\,\mathrm{d}t$$

$$S_{\text{inc}}^{\alpha}(\boldsymbol{Q}, \omega) = \frac{1}{2\pi}\int_{-\infty}^{\infty} I_{\text{inc}}^{\alpha}(\boldsymbol{Q}, t)\exp(-\mathrm{i}\omega t)\,\mathrm{d}t$$

the intermediate function for α and β species:

$$I^{\alpha\beta}(\boldsymbol{Q}, t) = \frac{1}{\sqrt{N_\alpha N_\beta}} \sum_{i_\alpha=1}^{N_\alpha}\sum_{j_\beta=1}^{N_\beta} \langle \exp\{\mathrm{i}\boldsymbol{Q}\cdot\boldsymbol{R}_{i_\alpha}(t)\} \times \exp\{-\mathrm{i}\boldsymbol{Q}\cdot\boldsymbol{R}_{j_\beta}(0)\}\rangle$$

$$I_{\text{inc}}^{\alpha}(\boldsymbol{Q}, t) = \frac{1}{N_\alpha}\sum_{i_\alpha=1}^{N_\alpha} \langle \exp\{\mathrm{i}\boldsymbol{Q}\cdot\boldsymbol{R}_{i_\alpha}(t)\} \exp\{-\mathrm{i}\boldsymbol{Q}\cdot\boldsymbol{R}_{i_\alpha}(0)\}\rangle.$$

Quasielastic Neutron Scattering

Intermeiate scattering law

$$I_s(Q,t) = \frac{1}{N}\sum b_i^{2,inc}\langle \exp i[r_i(t) - r_i(0)\rangle$$

$r = d + \rho + u$

d: center of mass position

ρ: scattering center with respect to c.o.m

u: a small vibrational displacement around the average position

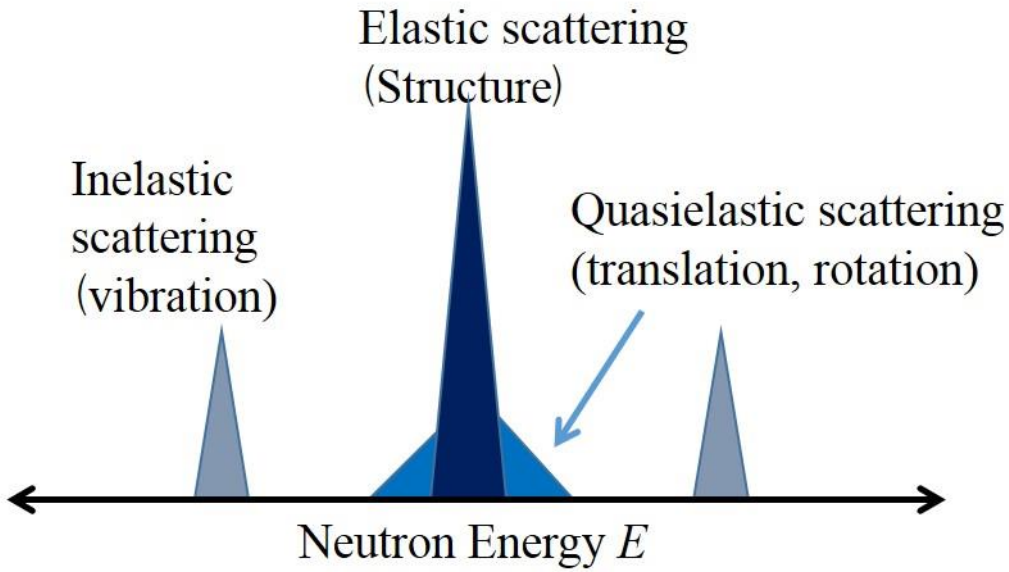

For uncoupled motions,

$$I_s(Q,t) = I_s^{trans} + I_s^{rot} + I_s^{vib}$$

By Fourier Transform

$$S_s(Q,\omega) = S_s^{trans} \otimes S_s^{rot} \otimes S_s^{vib}$$

$\otimes$ stands for the convolution product

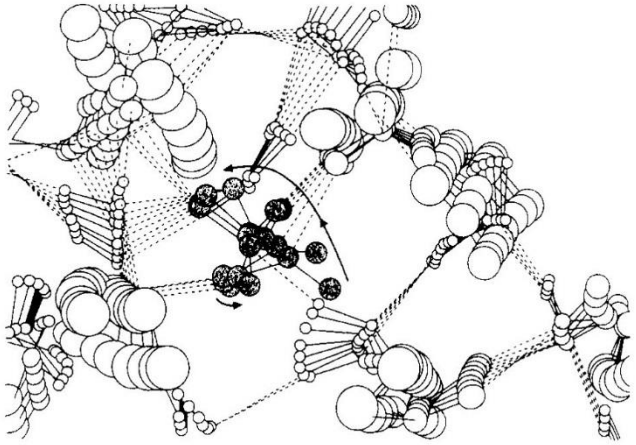

図 1　0.3 ps間のTIP2Pモデル水の動き[3)]

Vibrational part

$S_s^{vib} = I_s^{vib} = e^{-Q^2\langle U^2\rangle}$: Deby-Waller factor

$\langle U^2\rangle$: mean square amplitude of vibration

Translational part

When $Q \cdot a \ll 1$, where a is a molecular radius

$$I_s^{trans}(Q,t) = e^{-D_t Q^2 t}$$

D_t: self-diffusion coefficient

$$S_s^{trans}(Q,\omega) = \frac{1}{\pi}\frac{D_t Q^2}{(D_t Q^2)^2+\omega^2}$$

Full width at half maximum (FWHM) = $2D_t Q^2$

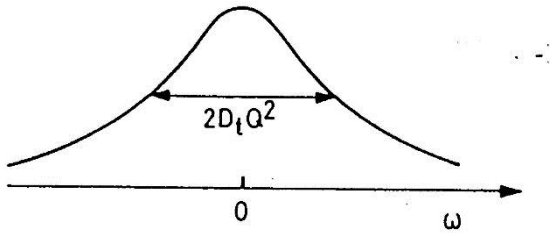

In case of $Q^2 < 0.1$
-Fick's law

HWHM=$D_t Q^2$

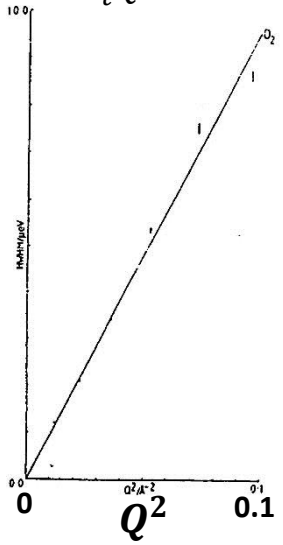

In case of $0.1 < Q^2 < \sim 2$
Random jump diffusion model

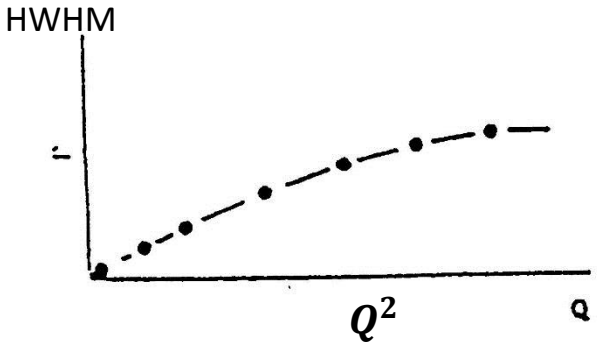

HWHM=$\frac{D_t Q^2}{1+D_t Q^2 \tau_0}$

$\tau_0 = \frac{\langle L^2\rangle}{6D_t}$

τ_0: residence time
L: jump distance

Rotationa part

Rotational diffusion on a sphere of radius a

$$S_s^{rot}(Q,\omega) = j_0^2(Qa)\delta(\omega) + \sum_{l=1}^{\infty}(2l+1)j_l^2(Qa)\frac{1}{\pi}\frac{l(l+1)D_r}{[l(l+1)D_r]^2+\omega^2}$$

$$I_s(Q,0) = \int_{-\infty}^{+\infty} S_s^{rot}(Q,\omega)d\omega$$

D_r: rotational diffusion constant

Spherical Bessel functions $j_l(Qa)$

$$\sum_{l=0}^{\infty}(2l+1)j_l^2(Qa) = 1$$

$$j_0(Qa) = \frac{\sin(Qa)}{Qa}, \quad j_1(Qa) = \frac{\sin(Qa)}{(Qa)^2} - \frac{\cos(Qa)}{Qa}$$

Institut Laue-Langevin (ILL), Grenoble, France
Beam lines & Inelastic Scattering Spectrometers

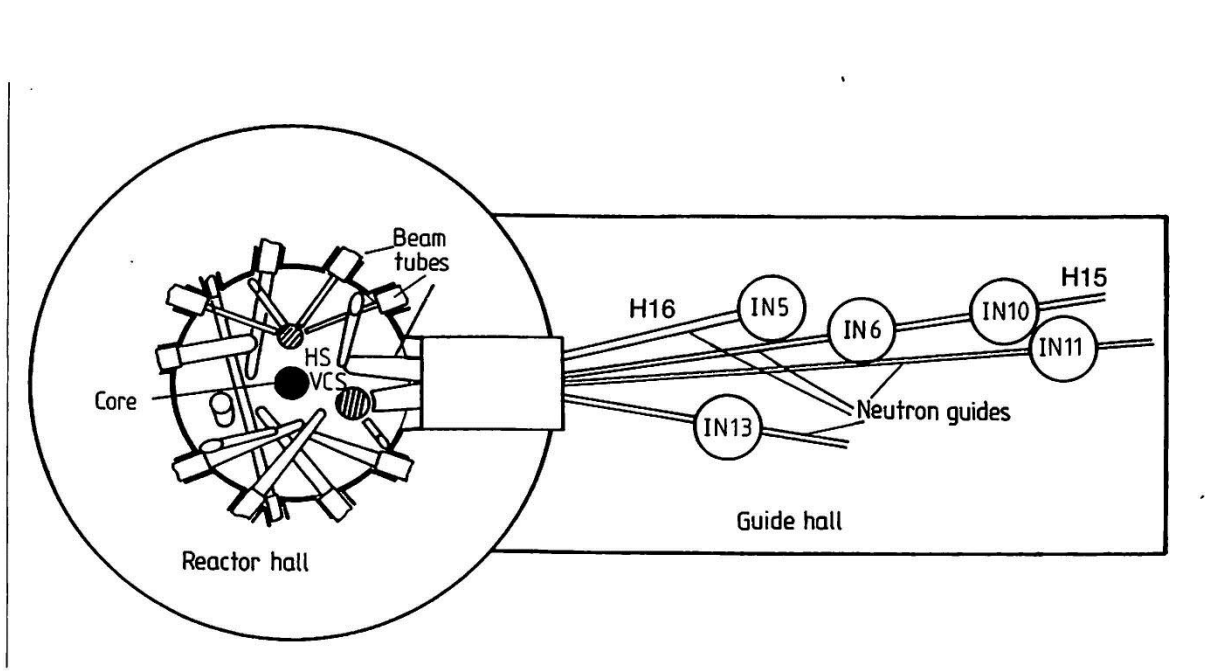

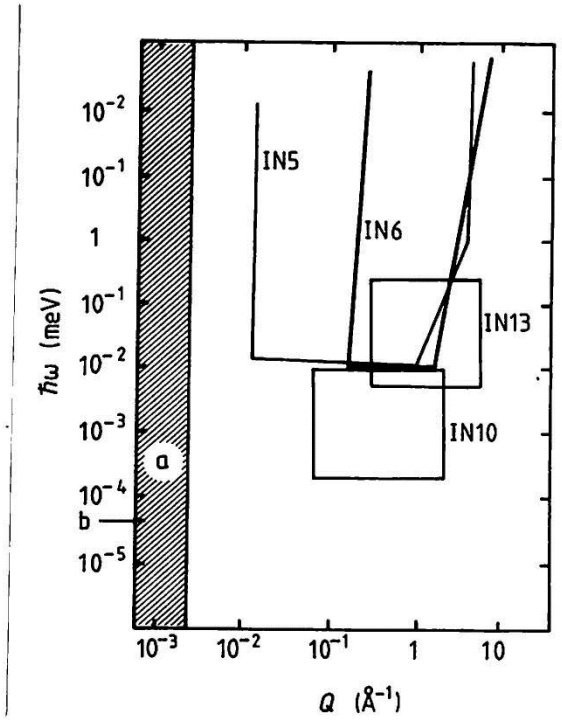

Time-of-Flight multichopper spectrometer IN5 at ILL

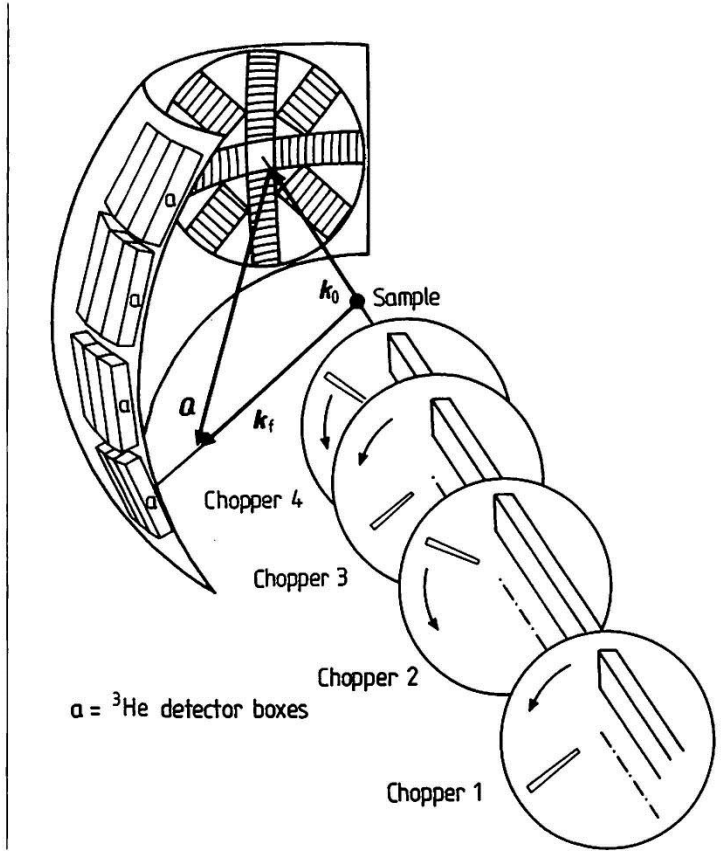

Choppers 1 and 4 determine the wavelength.
Chopper 2 eliminates higher-order neutrons.
Chopper 3 controls the repetition rate of the neutron bursts.
Chopper speed: 6000 ~ 20 000 rpm

Backscattering spectrometer IN10 at ILL

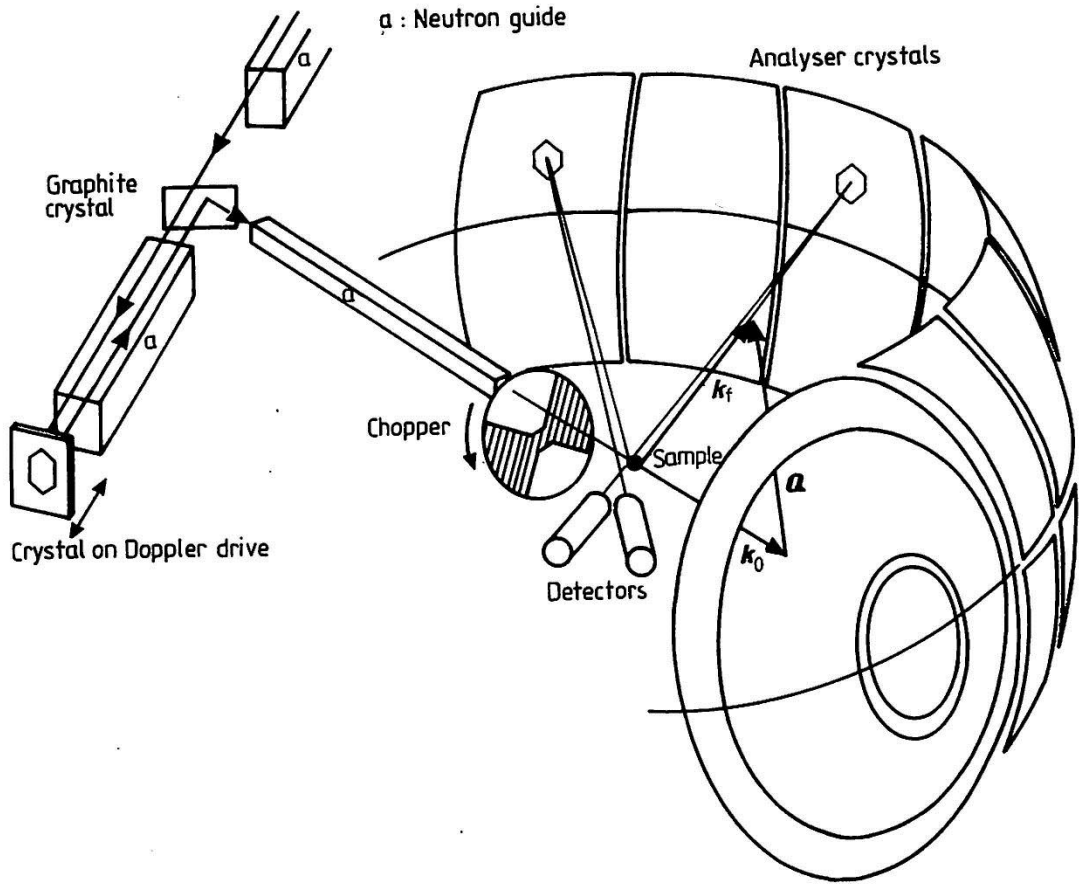

The neutron beam is backscattered by the monochromator mounted on a Doppler drive, deflected to the sample, scattered to the analysers and then backscattered again the detectors.

J-PARC MLF Beam Lines & Spectrometers

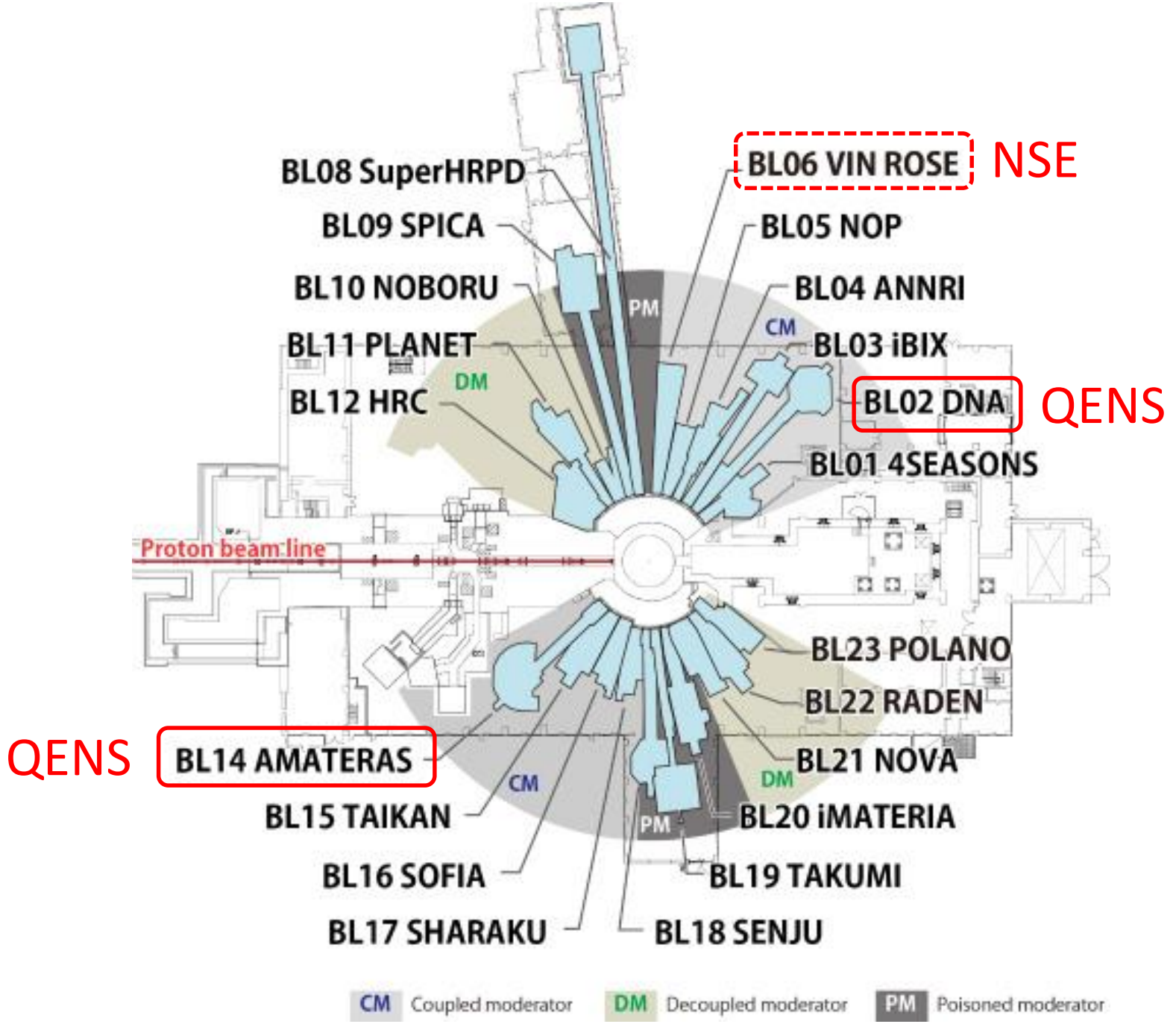

AMATERAS - Cold-Neutron Disk-Chopper Spectrometer -

AMATERAS Makes Revolution

Inelastic & Quasielastic Scattering Measurements in Low Energy Region with *High-Intensity*, *High-Resolution* and *High-Flexibility*

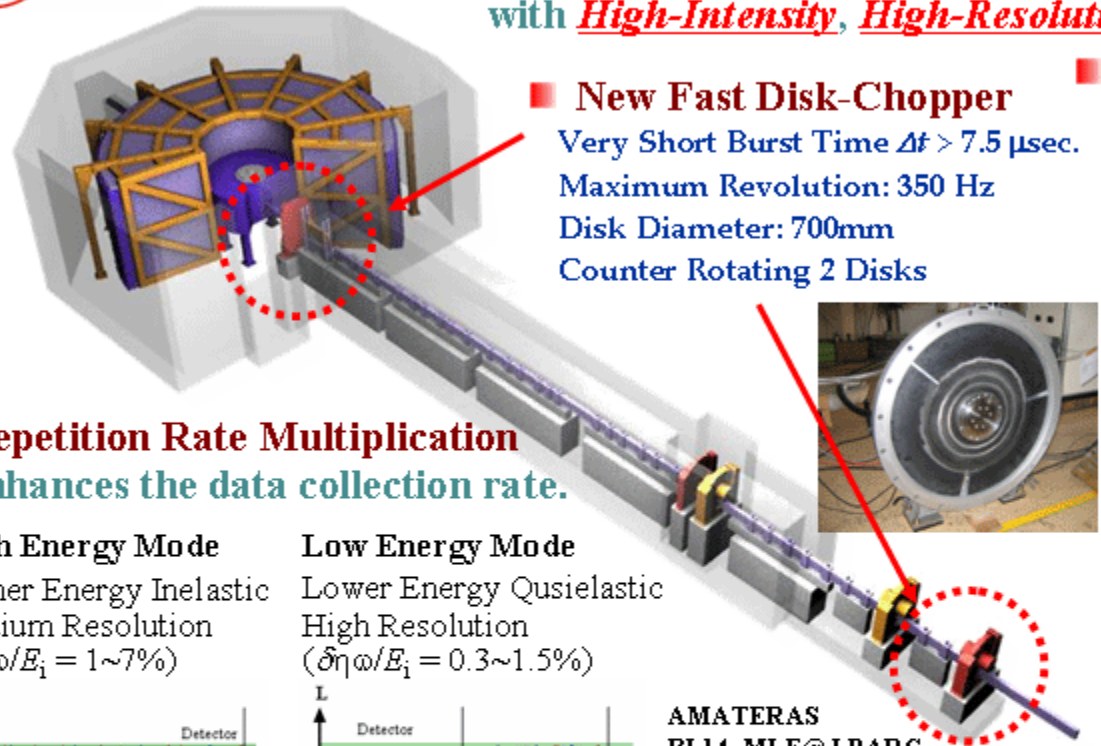

New Fast Disk-Chopper

Very Short Burst Time Δt > 7.5 μsec.
Maximum Revolution: 350 Hz
Disk Diameter: 700mm
Counter Rotating 2 Disks

Double-Chopper Spectroscopy @ Coupled Moderator Source

- Enjoy high peak-intensity of a coupled moderator without degrading the resolution by shaping a bad pulse profile.
- Pulse width (resolution) can be tuned.

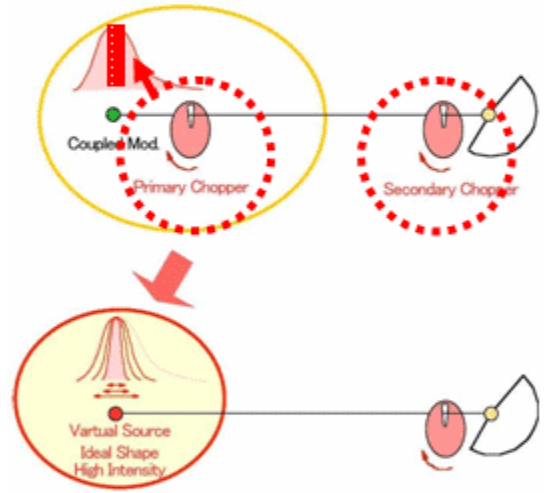

Repetition Rate Multiplication enhances the data collection rate.

High Energy Mode
Higher Energy Inelastic
Medium Resolution
($\delta\eta\omega/E_i = 1\sim7\%$)

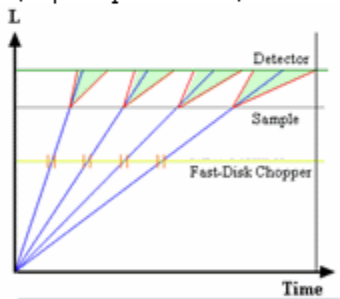

Low Energy Mode
Lower Energy Qusielastic
High Resolution
($\delta\eta\omega/E_i = 0.3\sim1.5\%$)

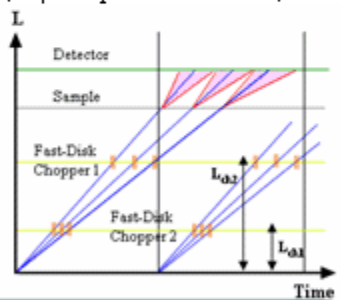

AMATERAS
BL14, MLF@J-PARC
Contact: Kenji Nakajima (J-PARC Center)
kenji.nakajima@j-parc.jp

APPLICATIONS

- Collective Excitations in Strongly Correlated Systems
- Dynamical Properties of Random Media such as Glass, Liquid, Polymer & etc...
- Diffusive Process in pico-sec. Time Scale

SPECIFICATION

- Coupled H_2 Moderator (liquid H_2)
- Flight Path: L_1=30 m, L_2=4 m
- Incident Neutron Energy: $1 \le E_i \le 80$meV
- Scattering Angle: -40° ~ 140° (Horizontal), -16° ~ 23° (Vertical)
- Momentum Resolution: $\delta Q/k_i$~1%
- Energy Resolution: $\delta\eta\omega/E_i \ge 1\%@E_i$=20meV, Easily Tunable
- Flux at Sample: 4×10^5 n/cm^2/sec.@$\delta\eta\omega/E_i = 3\%$, E_i=20meV
- Detector System: ^{3}He 1D-PSD ϕ=1" 10 atm L=3m, Ω=0.7π Sr

BL02 DNA: Dynamics Spectrometer

DNA is a High Energy Resolution Near-Backscattering Spectrometer

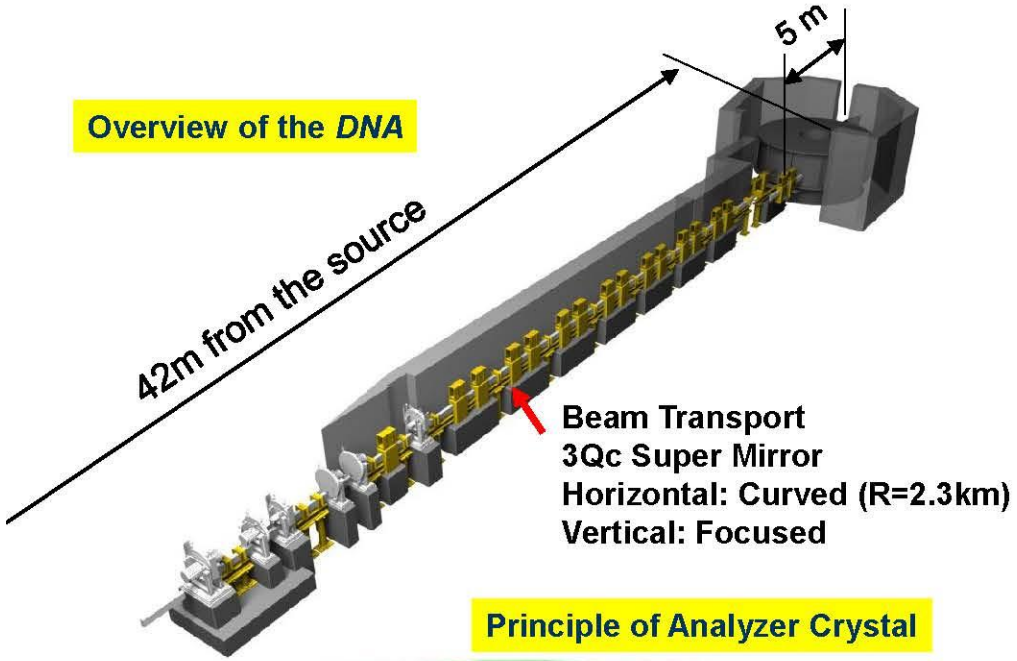

Source: Liq.H_2 Coupled Moderator (BL02)
Moderator-Sample:L_1 = 42 m
Sample-Detector: L_2 = 4.3 m,
Pulse-shaping device: L_{ch} = 7.75 m
Analyzer Bank: Spherical (R=2.3m)
Si(111)&Si(311)@θ_B=87.5 [deg.]
Si(111) :δE = 1.6 μeV, Q_{max} = 1.9 Å^{-1}@elastic
Si(311) :δE = 7 μeV, Q_{max} = 3.8 Å^{-1}@elastic
Horizontal Scat. Ang.:-164. < $2\theta_S$ < +164.[deg]
Vertical Scat. Ang.: -14. < $2\theta_S$ < +20.[deg]
High efficiency by RRM

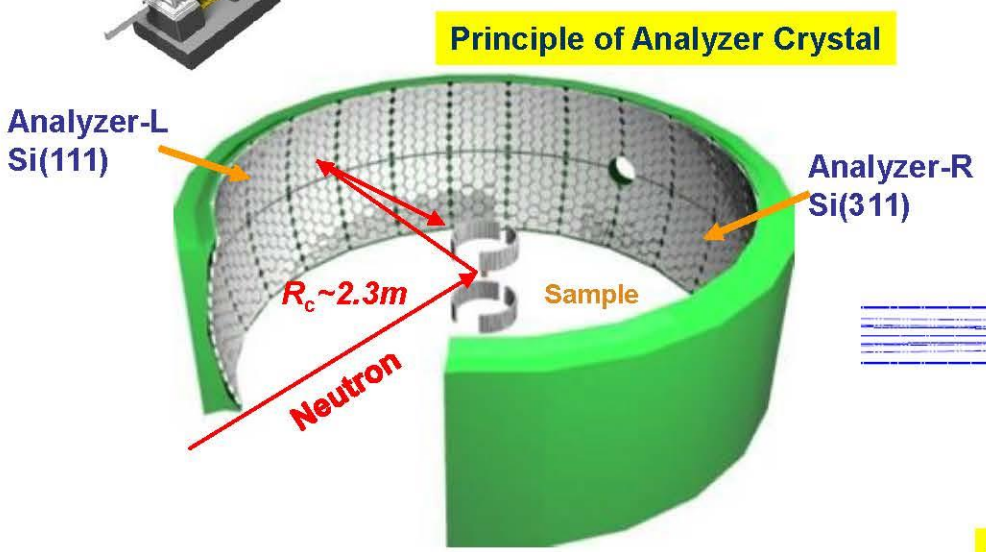

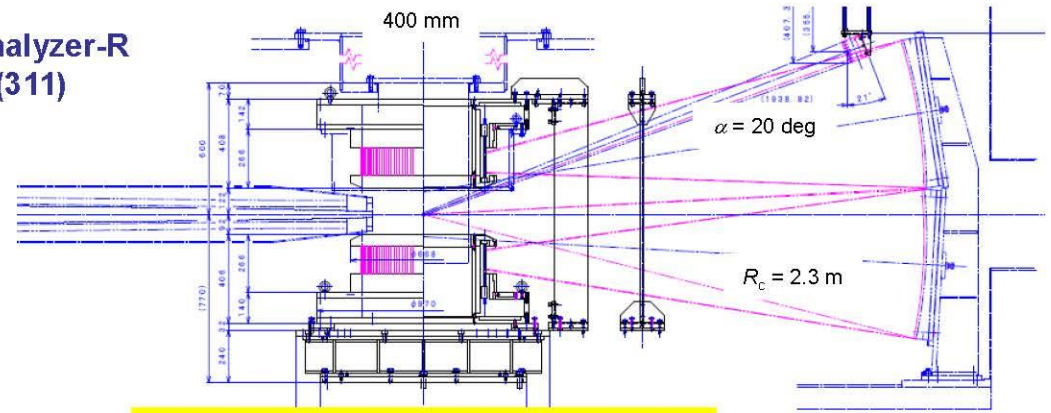

Section view of the scattering vessel

Confined water in Sephadex G-15

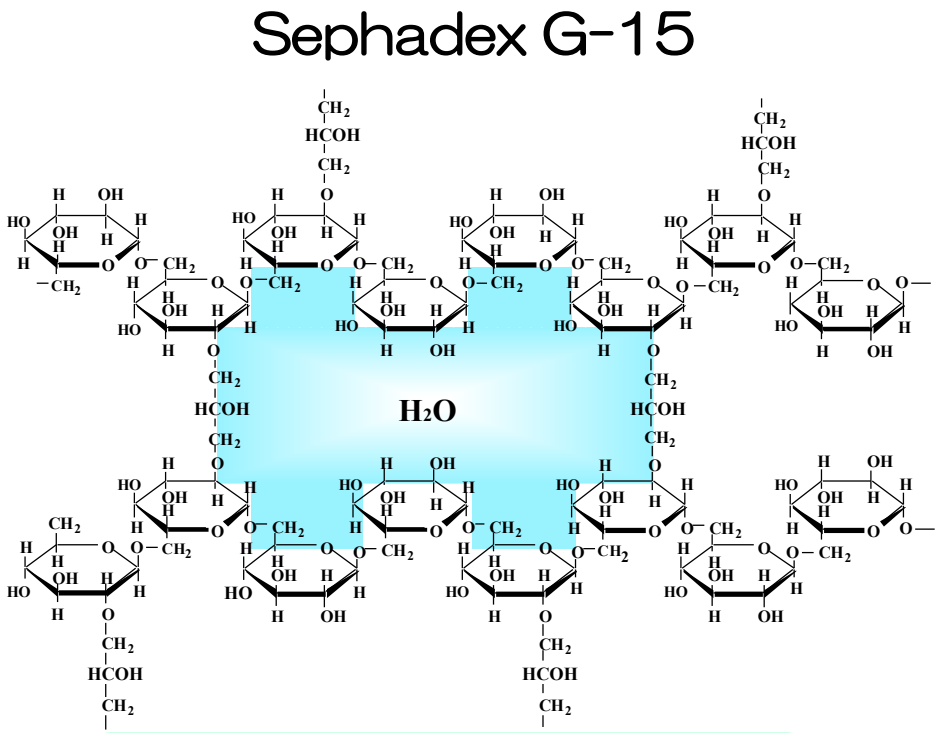

Schematic Representation of Sephadex G-type Gels

- Flexible polymer gels with amphiphilic interface → model for biological cell
- Network structure with inhomogeneous pores

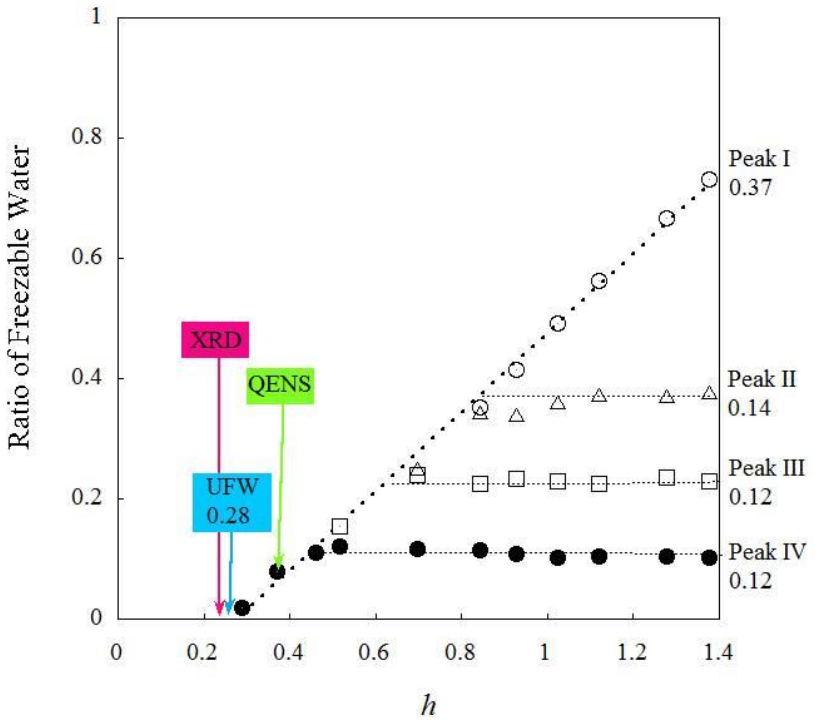

Bulk-like water (peak I)

Freezable bound water (FBW) (peaks II, III, and IV)

FBW II, III and IV might be formed due to strength of interaction with the substrate.

Unfrozen water (UFW) at $h < 0.28$

Dynamics of confined water in G15 gel by QENS

K. Ito, K. Yoshida, M.C.-Bellissent-Funel, T.Y. BCSJ, 87, 603 (2014).

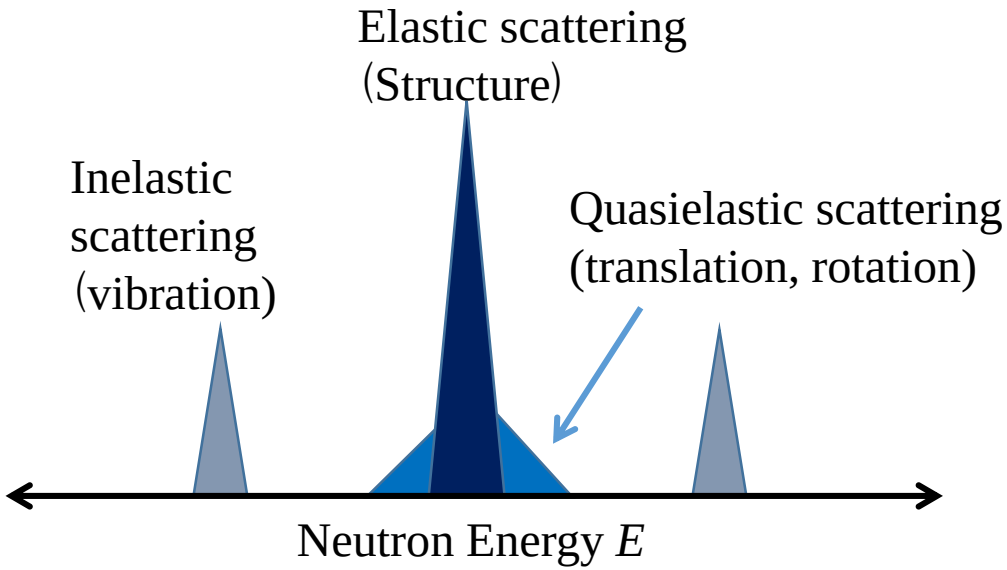

QENS experiments

on NEAT (Time-of-Flight) @:Helmholtz-Zentrum Berlin
λ= 7.1 Å, *Q*: 0.2 – 1.3 Å^{-1}, *E*:±0.6 meV
ΔE :28.6meV, T:245-290 K
H_2O and D_2O adsorbed Sephadex G-15
(Hydration level *h*= 0.38)
Flat Al cell with 1mm in sample thickness

S(*Q*, *ω*) of confined water in gels (*h* = 0.38,*Q*= 0.67 Å^{-1})

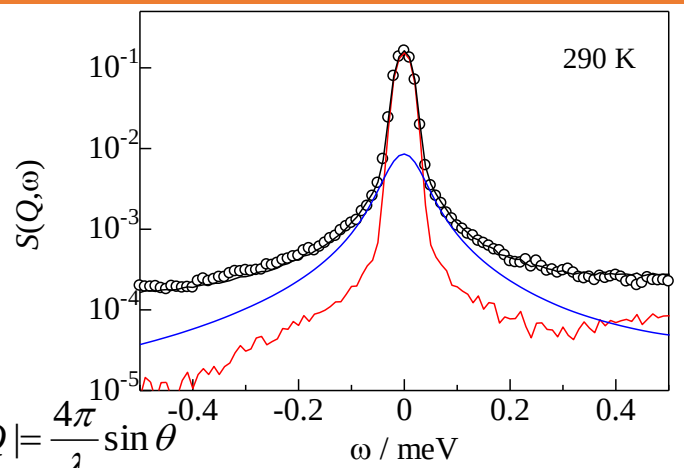

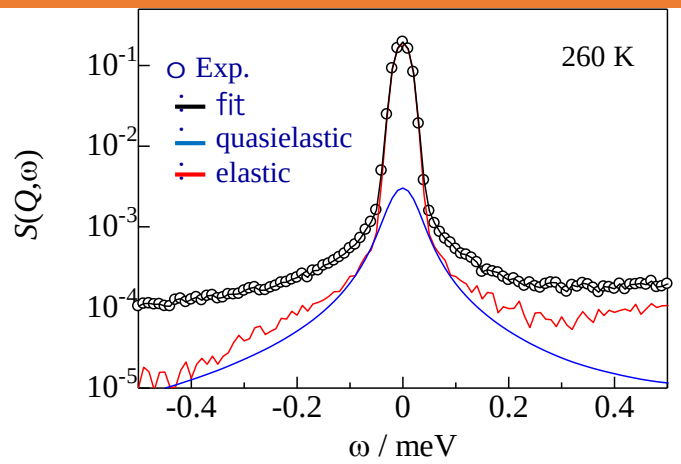

$$|Q| = \frac{4\pi}{\lambda}\sin\theta$$

$$S_S(Q,\omega) = (A_1(Q)\delta(\omega) + A_2(Q)\frac{\Gamma(Q)}{\Gamma^2(Q)+\omega^2})$$

Self diffusion constants , *D* , （3.2×10^{-5} cm^2/s）larger by a factor of ~2 than those of bulk, MCM-41, Vycor, and smaller by a factor of 3 than that for OMC

Dynamics of confined water in G15 gel by QENS

K. Ito, K. Yoshida, M.C.-Bellissent-Funel, T.Y. BCSJ, 87, 603 (2014).

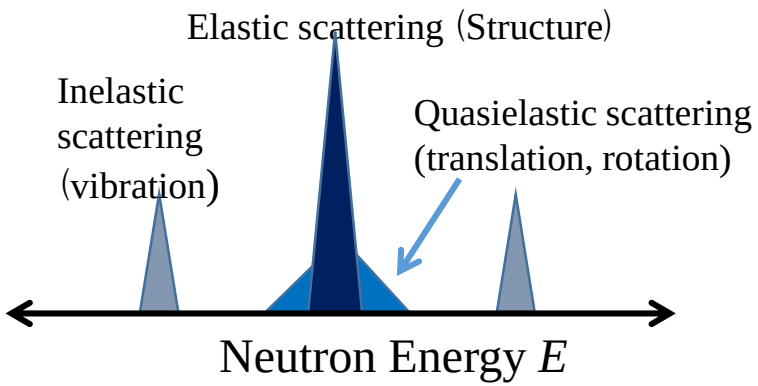

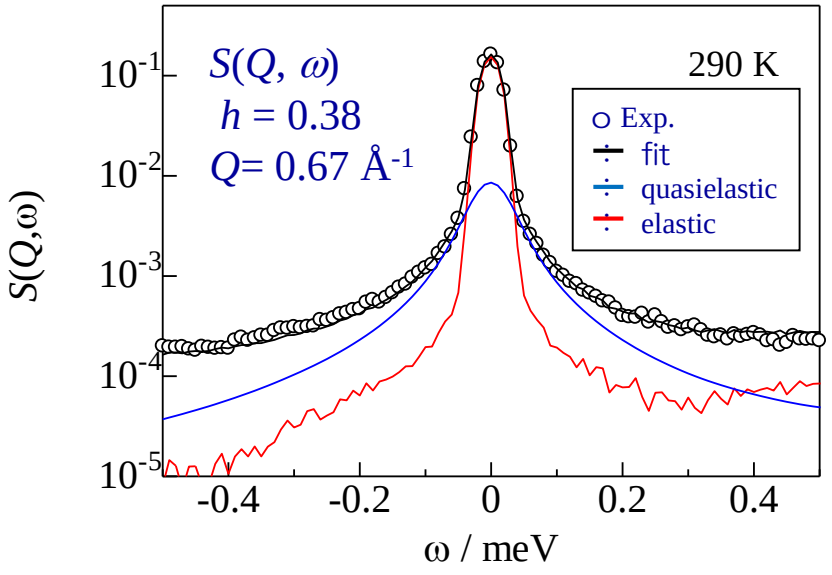

$$S_S(Q,\omega) = (A_1(Q)\delta(\omega) + A_2(Q)\frac{\Gamma(Q)}{\Gamma^2(Q)+\omega^2})$$

The water molecules perform local motions characterized by a diffusion coefficient D_{local} of (0.65 ±0.05) ×10^{-5} cm^2 s^{-1} in some volume estimated as a sphere with a radius of 4.4Å.

The activation energy of 44.2 ±1.5 kJ mol^{-1}, which is somewhat larger than the value (15~36 kJ mol^{-1}) of water in MCM-41 C10. Water molecules in G15 gel are strongly bound to the hydroxy groups of the crosslinked substrates.

Elastic Incoherent Structure Factor*1 (EISF)

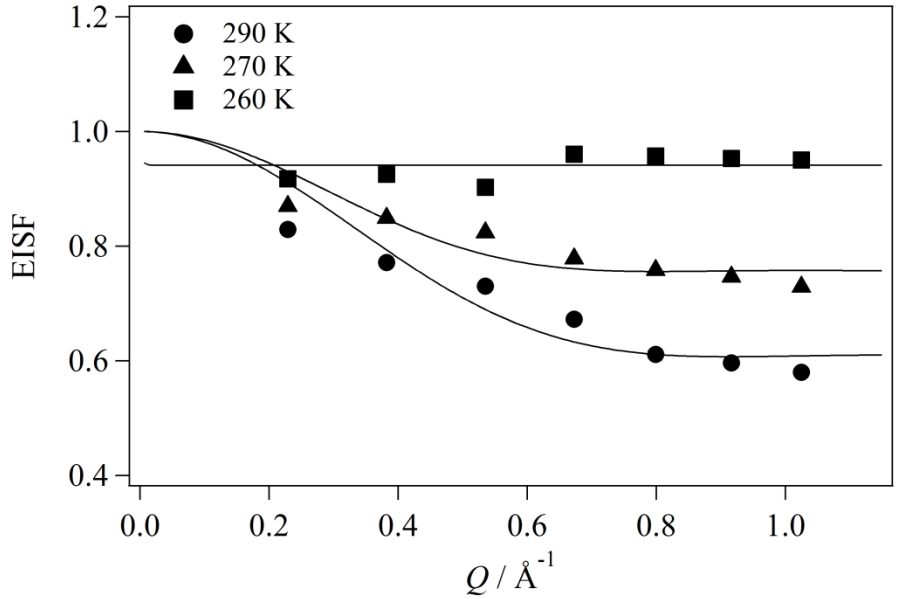

$$\mathrm{EISF} = \frac{I_{EL}}{I_{EL} + I_{QE}} = \left[\frac{3j_1(Qa)}{Qa}\right]^2 (1-p) + p$$

a: Radius of sphere p: elastic component

*1 F. Volino & A. J. Dianoux, Molecular Physics 41(2) (1980)271-279

T (K)	*P*	a (Å)
290	0.61±0.03	4.9±0.6
275	0.76±0.02	5.6±0.8

K. Ito, K. Yoshida, M.C.-Bellissent-Funel, T.Y. BCSJ, 87, 603 (2014).

Water confined in mesoporous silica

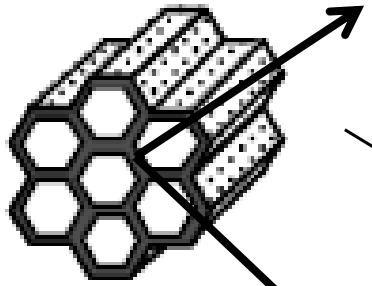

non-modified

MCM-41 C41

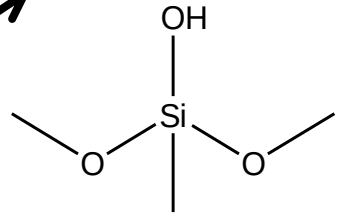

- **pore diameter 28 Å**
- **pore volume 0.926 cm^3 / g**
- **surface area 1300 m^2/g**

modified

Ph-PMO

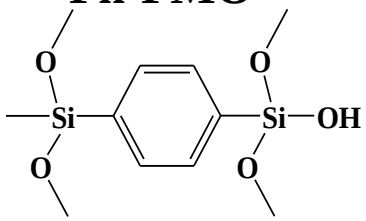

- **pore diameter 27 Å**
- **pore volume 1.00 cm^3 / g**
- **surface area 2309 m^2/g**

Bp-PMO

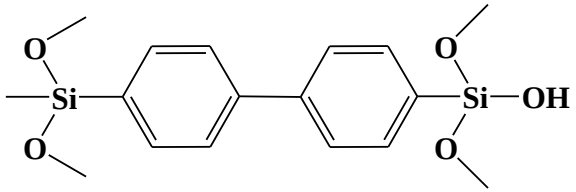

- **pore diameter 25 Å**
- **pore volume 0.459 cm^3 / g**
- **surface area 805 m^2/g**

TMS-Ph-PMO

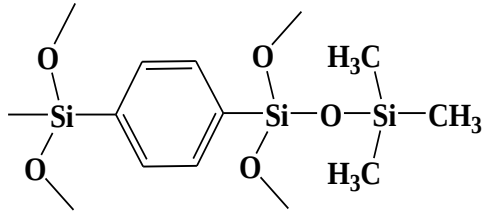

- **pore diameter 27 Å**
- **pore volume 1.04 cm^3 / g**
- **surface area 2089 m^2/g**

Hydrophobicity

Do dynamic properties of confined water change with increasing hydrophobicity of pore wall?

Water adsorption and desorption isotherms at 295 K

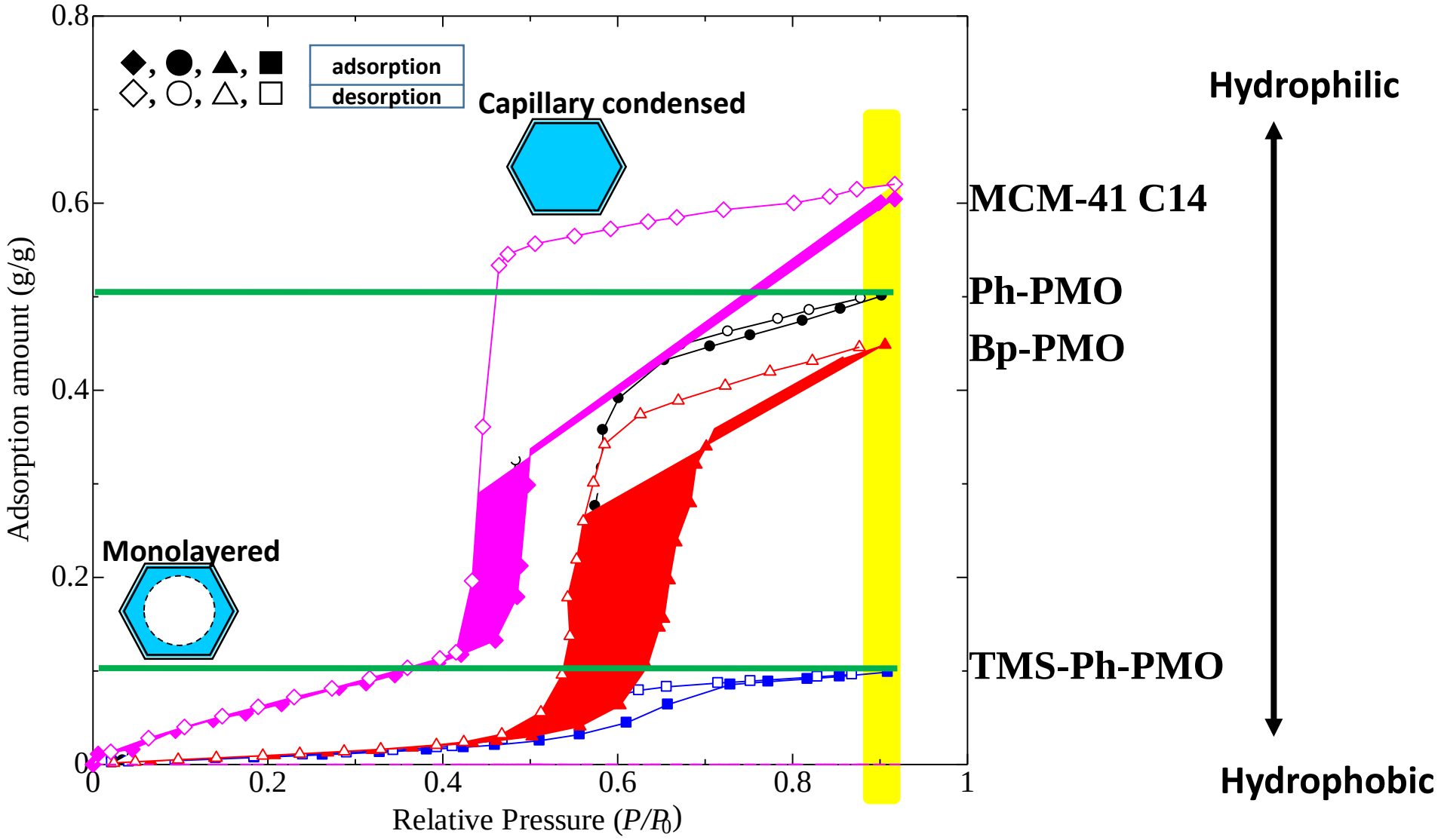

MCM-41 C14 data : Kittaka@OUS

QENS spectra of confined water at Q = 1.6 Å^{-1}

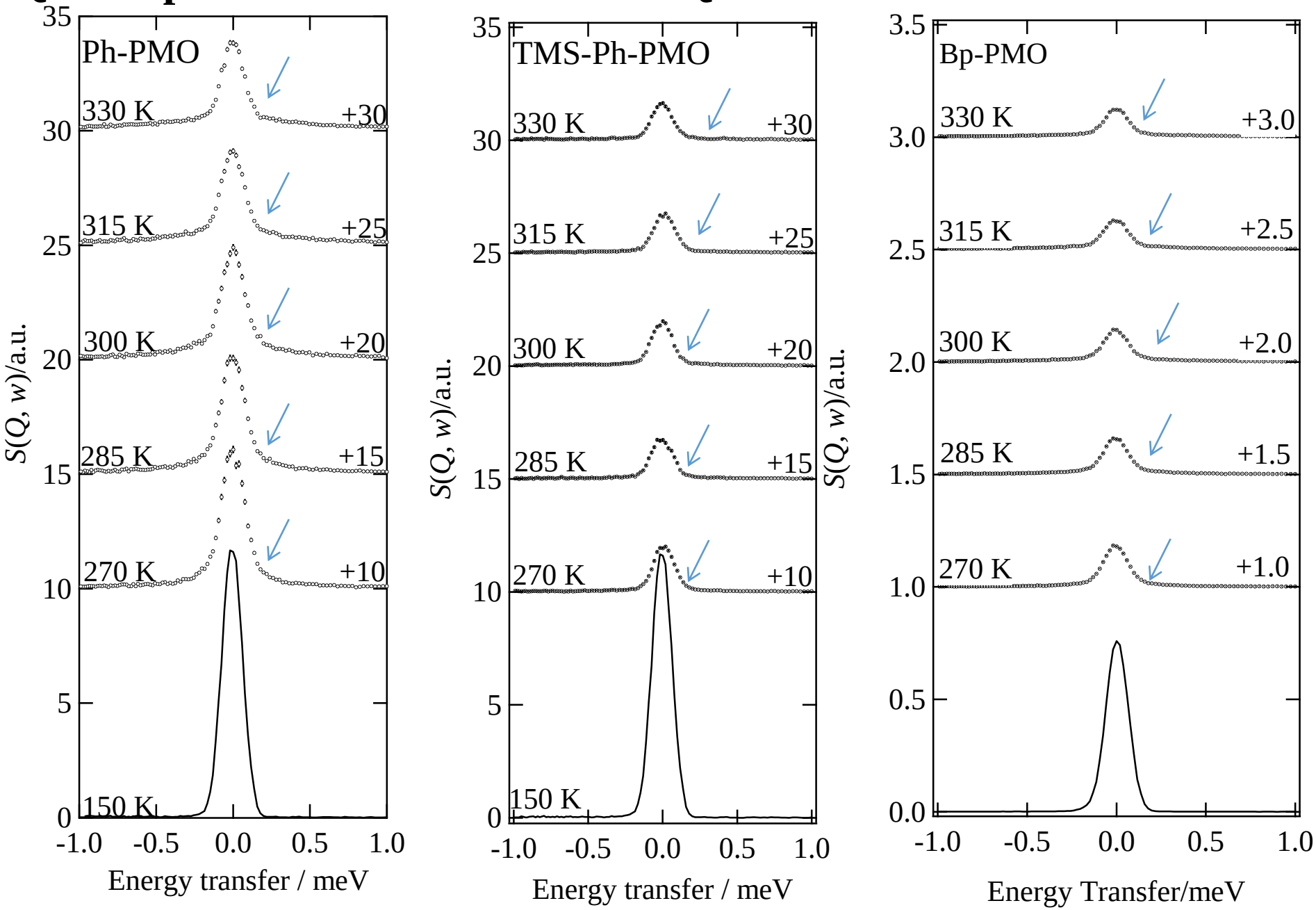

Analysis by the Teixeira method

J. Teixeira, M.-C. Bellissent-Funel, S. H. Chen, and A.J. Dianoux, *Phys. Rev. A*, **31**, 1913 (1985).

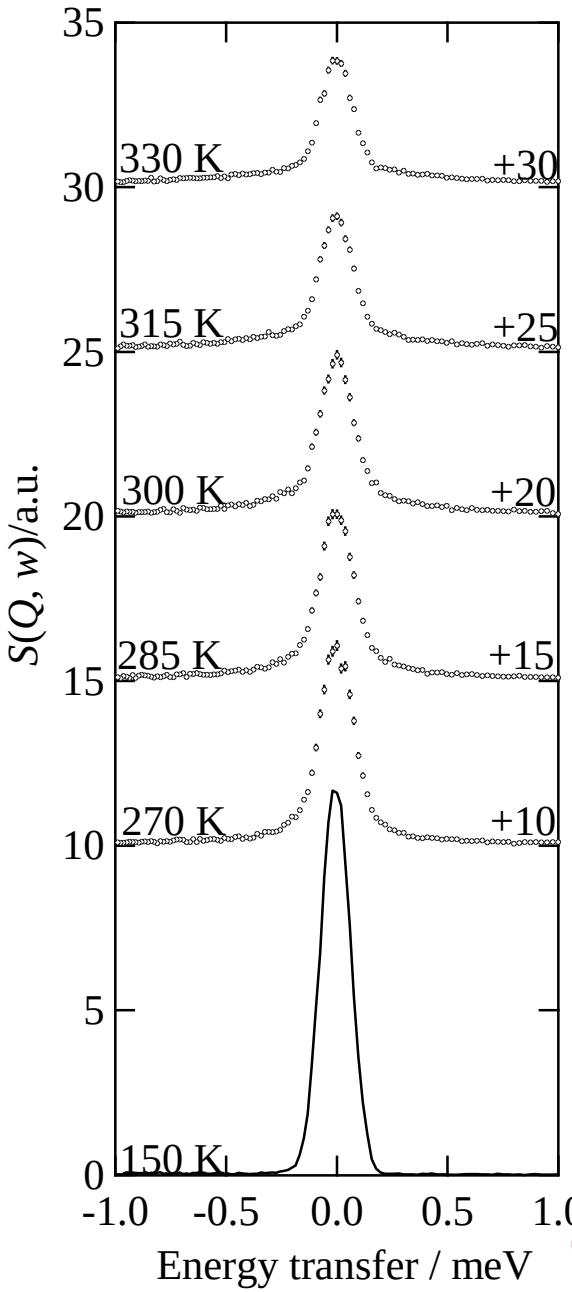

Fitting

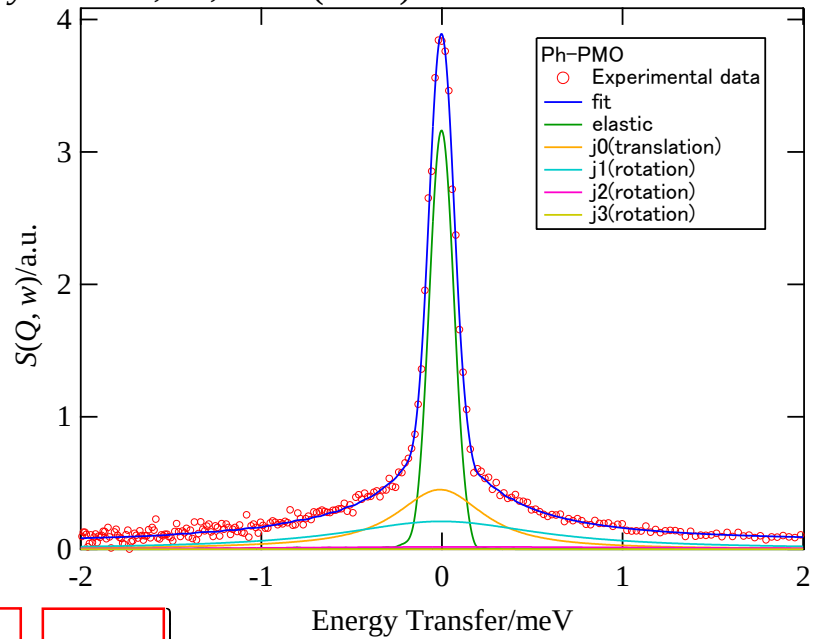

$$S(Q,\omega)=\left\{\delta(\omega)+\exp\left(-\frac{Q^2\langle u\rangle}{3}\right)^2 L_{\mathrm{Trans}}(Q,\omega)\otimes L_{\mathrm{Rot}}(Q,\omega)\right\}\otimes R(Q,\omega)+BG$$

Translation

$$L_{\mathrm{Trans}}(Q,\omega)=\frac{1}{\pi}\left[\frac{\Gamma(Q)}{\omega^2+\Gamma(Q)^2}\right]$$

HWHM

$$\Gamma(Q)=\frac{DQ^2}{1+DQ^2\tau_0}$$

Rotation

$$L_{\mathrm{Rot}}(Q,\omega)=j_0^2(Qa)\delta(\omega)+\frac{1}{\pi}\sum_{l=1}^{\infty}(2l+1)j_l^2(Qa)\frac{l(l+1)D_{\mathrm{rot}}}{\omega^2+\left[l(l+1)D_{\mathrm{rot}}\right]^2}$$

Relaxation time

$$\tau_1=\frac{1}{6D_{\mathrm{rot}}}$$

Arrhenius plots of diffusion coefficient and relaxation time of confined water

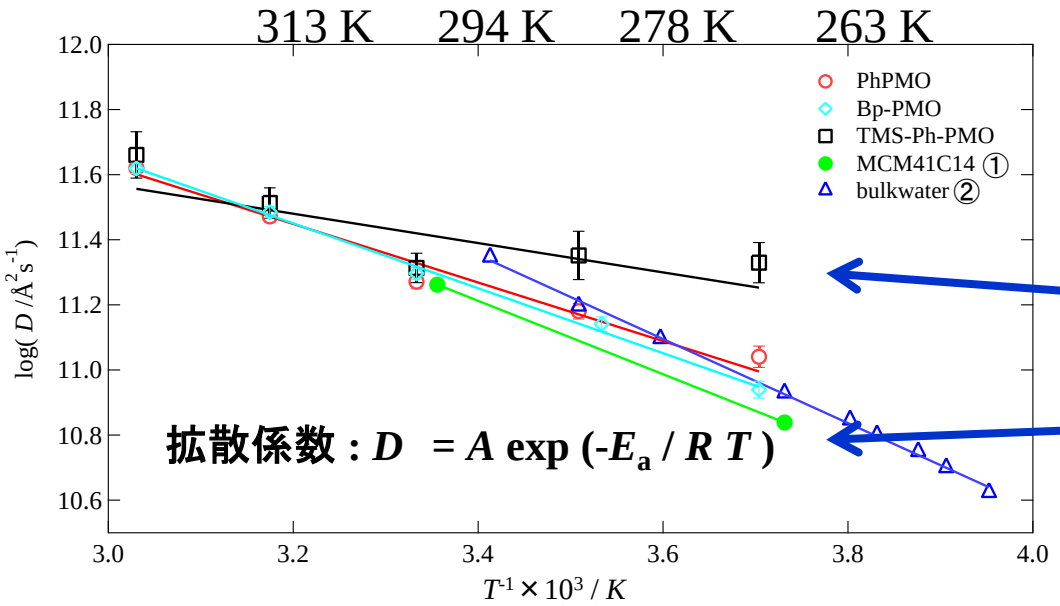

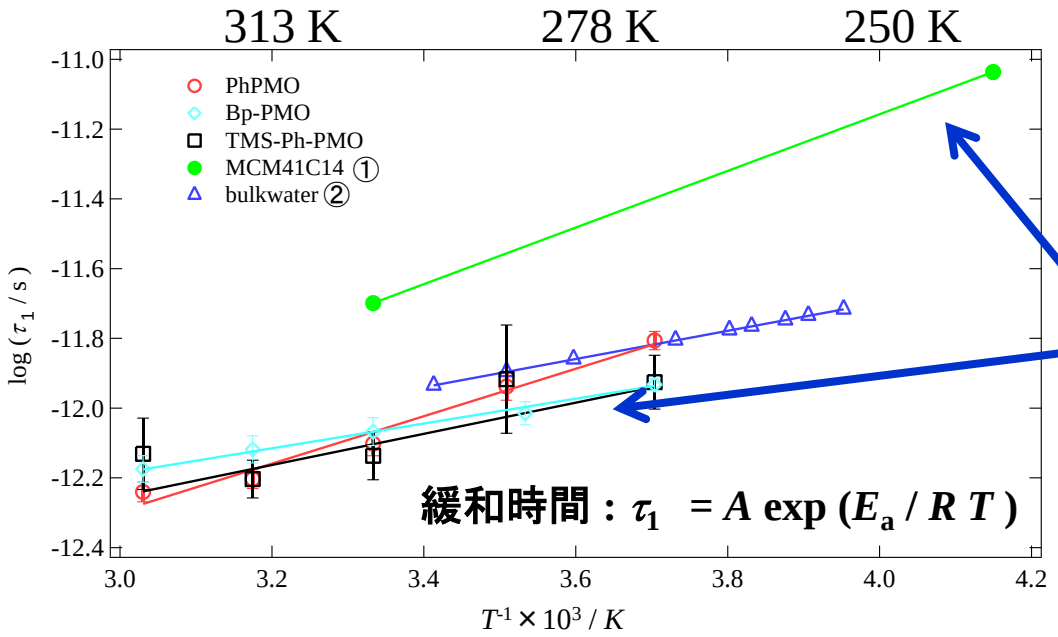

<Diffusion coefficient>

Diffusion coefficient increases with increasing hydrophobicity

TMS-Ph-PMO water
Most diffusable
MCM-41 C14 water
Least diffusable

<Relaxation time>

Relaxation time decreases with increasing hydrophobicity

TMS-Ph-PMO water
Fastest rotation
MCM-41 C14 water
Slowest rotation

①S. Takahara, M. Nakano, S. Kittaka, Y. Kuroda, T. Mori, H. Hamano and T. Yamaguchi, *J. Phys. Chem. B*, **103**. 5814 (1999).
② J. Teixeira, M.-C. Bellissent-Funel, S. H. Chen and A.J. Dianoux, *Phys. Rev. A*, **31**, 1913 (1985).

Activation energy of translational diffusion coefficient and rotational relaxation time

modified ⟷ non modified

	Bulk water①	TMS-Ph-PMO	Bp-PMO	Ph-PMO	MCM-41 C14②
Diffusion coefficient(kJ/mol)	17.9±0.9	8.64±2.28	19.1±0.7	17.2±0.9	21.6
		small ⟷			large

modified ⟷ non modified

	Bulk water①	TMS-P-PMO	Bp-PMO	Ph-PMO	MCM-41 C14②
Relaxation time (kJ/mol)	13.5±0.8	8.55±2.97	6.82±0.97	13.0±1.0	15.6
		small ⟷			large

- **A.E. of water in Ph-PMO is almost comparable with that of bulk water.**
- **Water confined in MCM-41 C14 diffuses and rotates with higher A.E. compared with bulk water.**
- **Water confined in TMS-Ph-PMO diffuses and rotates with lower A.E. compared with bulk water.**

① T. Yamada, R. Yonamine, T. Yamada, H. Kitagawa, M. Tyagi, M. Nagao and O. Yamamuro, *J. Phys. Chem. B*, **115**, 13563 (2011).

②S. Takahara, M. Nakano, S. Kittaka, Y. Kuroda, T. Mori, H. Hamano and T. Yamaguchi, *J. Phys. Chem. B*, **103**. 5814 (1999).

Jump Diffusion Model

A water molecule jumps by L after the residence time τ_0

$$< L >= (6 D \tau_0)^{1/2}$$

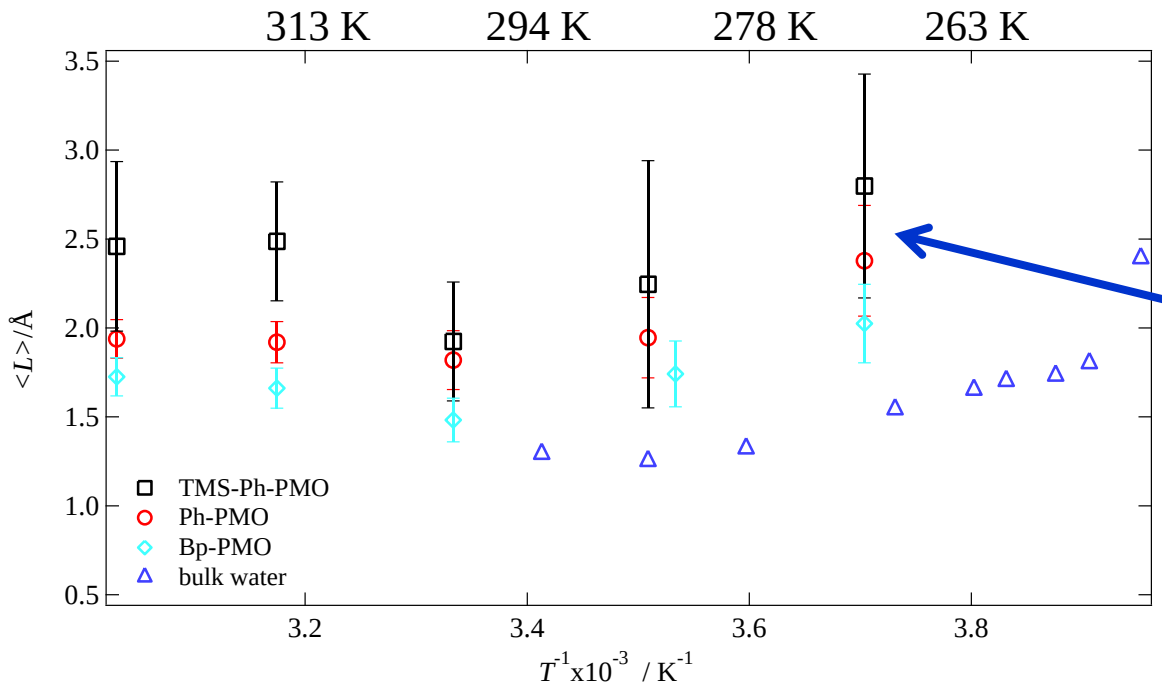

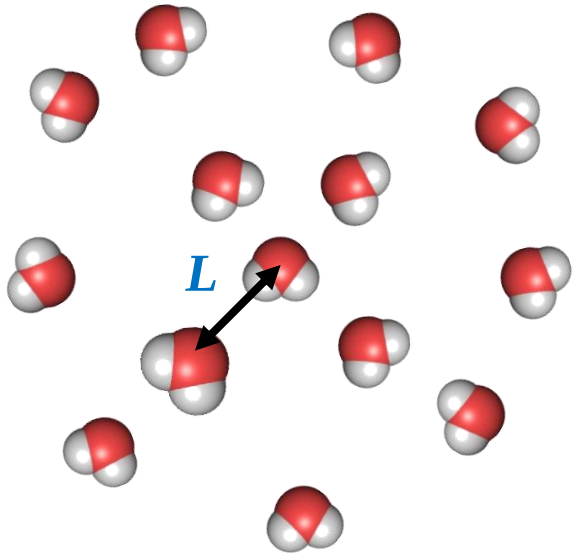

<Confined water>
Jump distance is longer compared with bulk water.

<TMS-Ph-PMO>
Longest jump distance

Bulk water data taken from

J. Teixeira, M.-C. Bellissent-Funel, S. H. Chen and A.J. Dianoux, Phys. Rev. A, **31**, 1913 (1985).

Neutron Spin-Echo

When neutrons with a spin of $\frac{1}{2}$ travel in a homogeneous magnetic field H_0, the neutrons perform Larmor precessions with angle ϕ.

$$\phi = \gamma_L \frac{lH_0}{v}$$

v: neutron velocity

γ_L: gyromagnetic ratio (2.916 kHzO$_e^{-1}$)

Polarization component, P_x, along a direction of x perpendicular to H_0 is

$$P_x = \langle cos\phi \rangle = \int f(v) cos \frac{\gamma_L l H_0}{v} dv$$

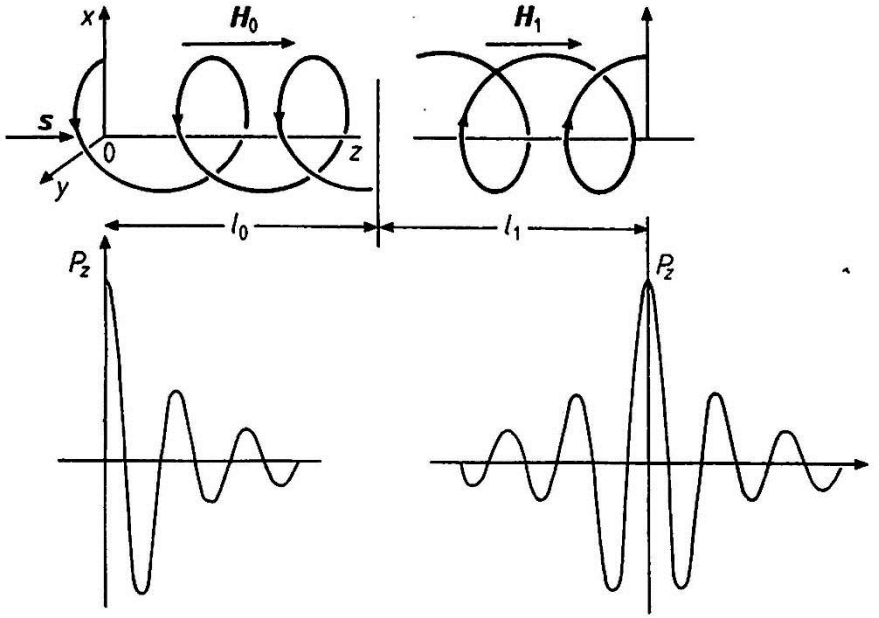

$$P_x = \langle \cos(\phi - \bar{\phi}) \rangle$$

$$= \frac{\int S(Q,\omega) \cos[t(\omega - \bar{\omega})]\, d\omega}{\int S(Q,\omega) d\omega}$$

$$= \frac{I(Q,t)}{I(Q,0)}$$

Normalized intermediate scattering function

Neutron spin echo technique measures inelastic scattering of water over energy E and length Q scale

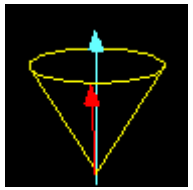

Neutron spins

Incident neutrons lose energy due to inelastic process for the motion of water.

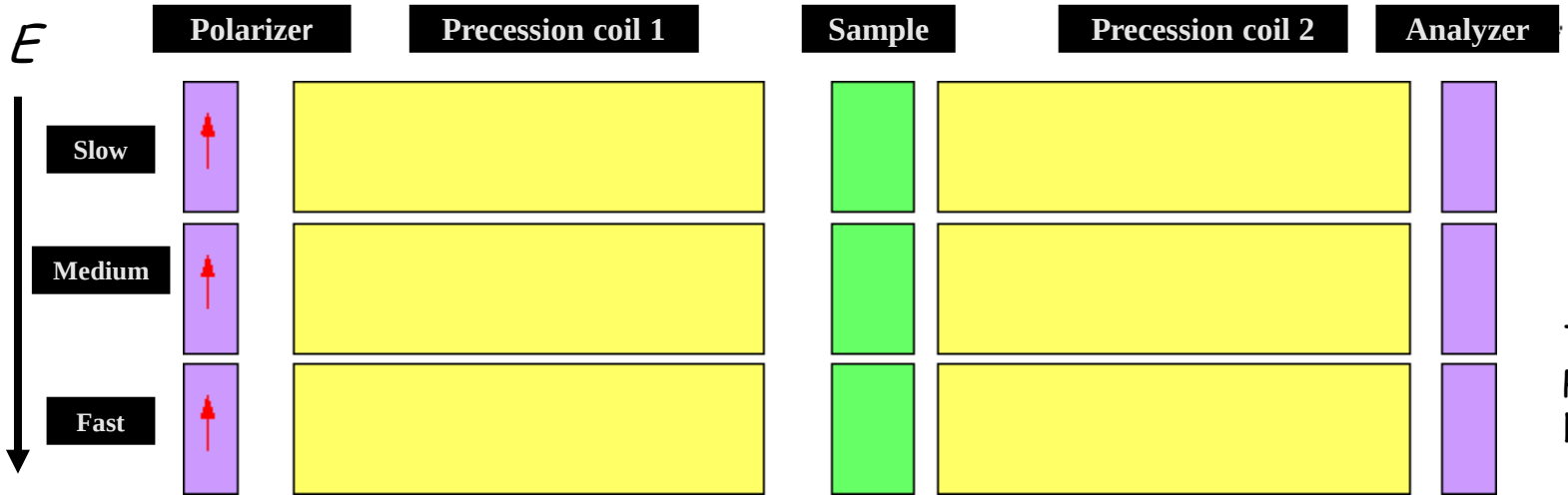

Taken from Prof. Seto's homepage

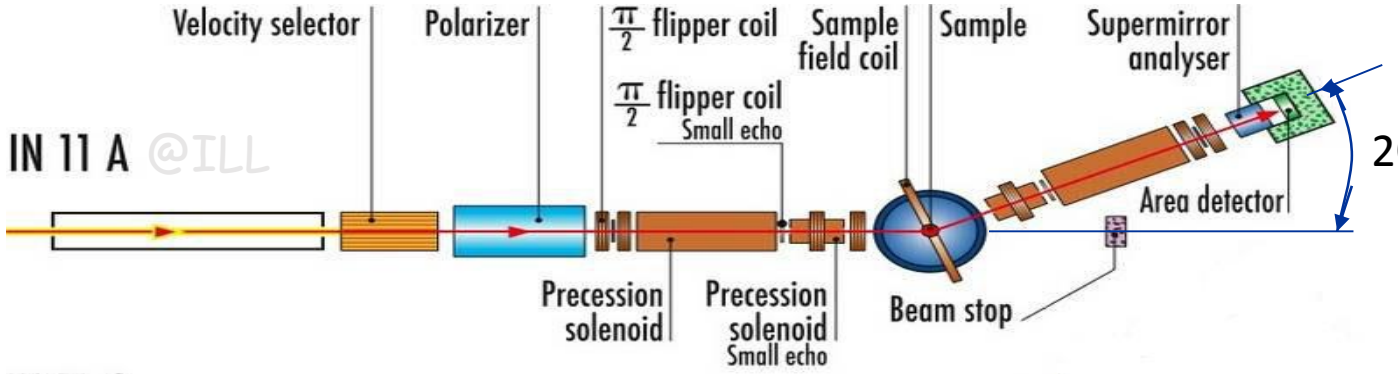

$Q = 4\pi \sin\theta/\lambda$

$= 2\pi/d$

Taken from ILL homepage

Intermediate scattering functions $I(Q,t)$ of CC D_2O confined in MCM-41 C10 obtained by NSE

Yoshida, TY, Kittaka, Bellissent-Funel, Fouquet, JCP, 129 (2008) 54702.

Q = 17 nm^{-1}

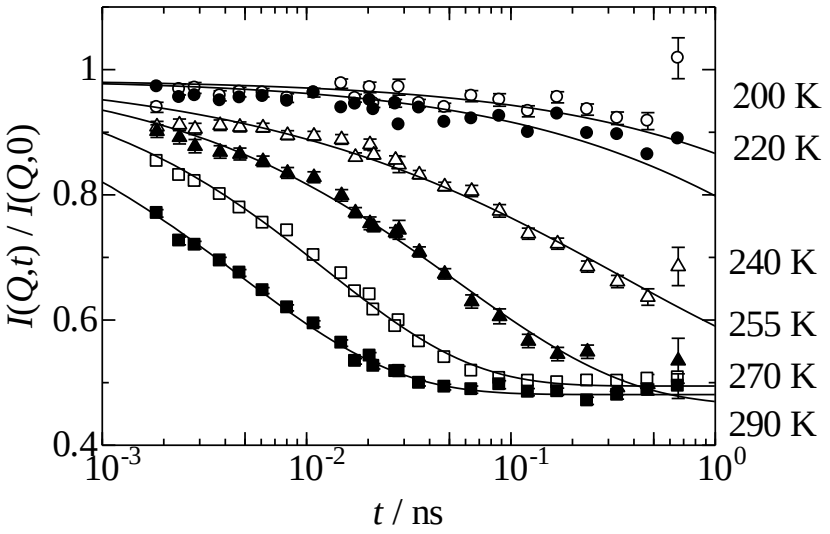

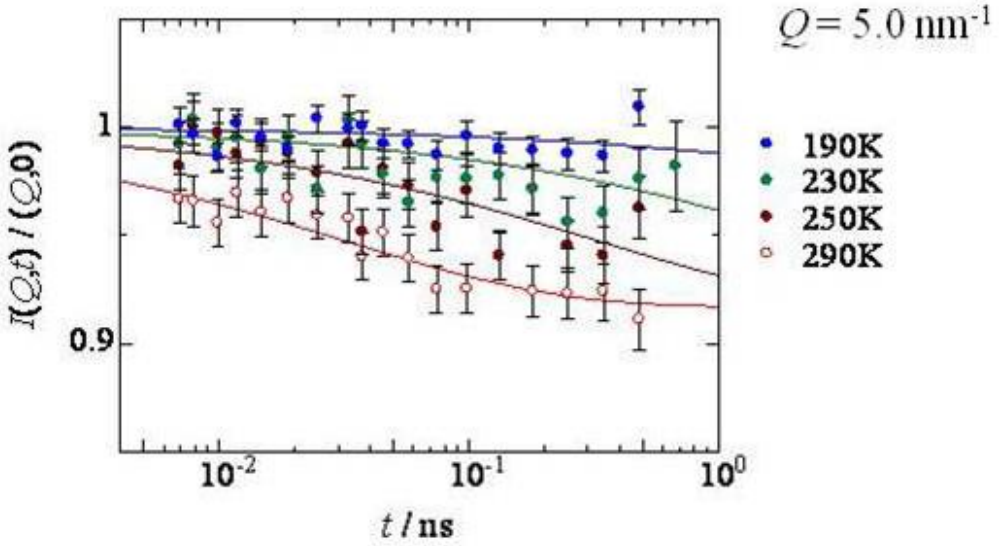

Kohlrausch-Williams-Watts (KWW) stretched exponential function

$$I(Q,t) = (1-p(Q))A(Q)\exp\left\{-\left(\frac{t}{\tau(Q)}\right)^{\beta(Q)}\right\} + p(Q)$$

$A(Q)$ Debye-Waller factor
$\tau(Q)$ relaxation time
$b(Q)$ stretched exponent
$p(Q)$ elastic term attributed to silica

Dynamic properties of water confined in MCM-41 C10

K. Yoshida, T.Y., S. Kittaka, M.-C. Bellissent-Funel, P. Fouquet, J. Phys.: Condens. Matter, 24, 064101 (2012)

Vogel-Fulcher-Tamman (VFT) equation

$$\tau(Q) = \tau_0(Q)\exp\left(\frac{D(Q)T_0(Q)}{T - T_0(Q)}\right)$$

$\tau_0(Q)$ pre-exponential factor
$D(Q)$ fragility
$T_0(Q)$ ideal glass transition temperature

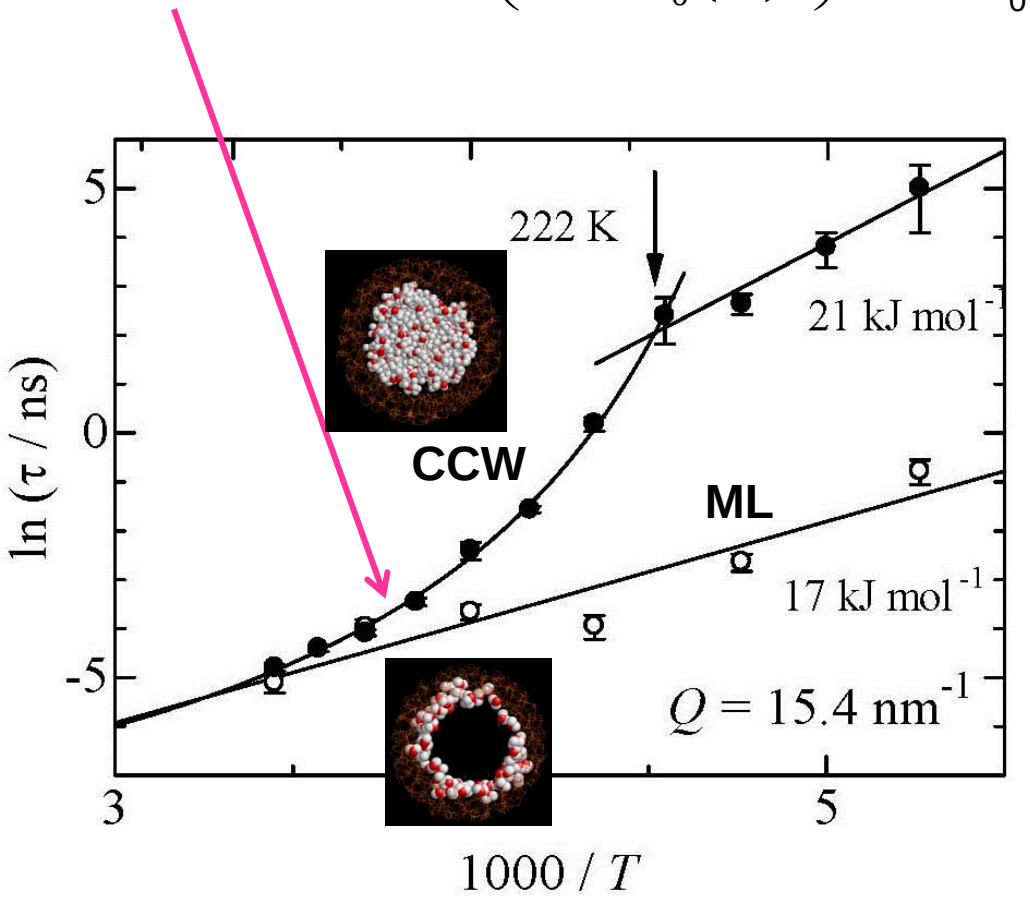

Monolayer water
Arrhenius type behaviour
<Ea> = 17 kJ/mol
Capillary condensed water
T>~220 K VFT behaviour
Fragile liquid
high density liquid
T<~220 K Arrhenius type
Strong liquid
low density liquid
<Ea> = 21 kJ/mol

α-relaxation to β-relaxation dynamical crossover arises from water in the central region of the pore.

Thank you for your kind listening

Bird-eye view of Fukuoka University